Proceedings of Global Power and Propulsion Society
ISSN-Nr: 2504-4400
GPPS Hong Kong 2023
October 17-19, 2023
www.gpps.global

GPPS-TC-2023-0051

Influence of film cooling hole geometry on the gas turbine blade strength

Tong Huang, Xinrong Su, Xin Yuan
Key Laboratory for Thermal Science and Power Engineering of Ministry of Education, Tsinghua University
suxr@mail.tsinghua.edu.cn
Beijing, China

ABSTRACT

Film cooling is an efficient method to protect gas turbine blade from high temperature gas under operation conditions nowadays. In most existing studies, the effects of hole geometry on the cooling performance are considered; however, the strength of turbine blade is also largely affected by the cooling holes, which lead to stress concentration on the blade surface and reduce the blade strength. In this paper, five basic geometry parameters of shaped film cooling hole are considered, including ratio of cylinder section length to total length, expansion angles at the leading edge and the trailing edge, the lateral angle and the radius of four edges inside diffuser. Based on these parameters, two composited variables are proposed, which have negative correlation with area average temperature and maximum von Mises stress respectively. By finding suitable basic parameters, the composited variables can be large at the same time, resulting in better performance of both cooling effect and structure strength.

INTRODUCTION

Gas turbine is a very important thermal power conversion machine based on Brayton cycle with very high efficiency. While to reach even higher efficiency, the inlet temperature of the turbine increase continuously and may exceed 2200 K for the next generation (Zhang et al., 2020). The hot-section components should be protected from the hot gas, otherwise the whole turbine could fail and leading to accident.

A basic method for protecting hot-section components is using film cooling, which transports cooler air from the compressor to the surfaces of hot-section components. At first, the the cooling hole is cylinder, while the kidney vortices caused by its geometry lead to a poor cooling effect. In 1970s, Goldstein et al (Goldstein et al., 1974) found that, the fan shaped cooling hole could provide better cooling air coverage than the cylinder hole. Since then, numerous researches paid attention on the fan shaped hole, hoping to provide deeper knowledge and better performance.

Yu et al (Yu et al., 2002) carried on an experiment with three different cooling hole shapes, and found that the hole with both forward and lateral diffusion had higher film effectiveness and lower heat transfer coefficient, comparing to cylinder hole. Gritsch et al (Gritsch et al., 2005) investigated influence of more hole geometry parameters on the thermal performance, including hole inlet-to-outlet area ratio, hole coverage ratio, hole pitch ratio, hole length and hole orientation angle. They found that these parameters had limited influence on the laterally average film-cooling effectiveness. Sargison et al (Sargison et al., 2002*a*,*b*) measured a new cooling hole, converging slot-hole or console, with fan shaped hole. According to their results, the laterally averaged heat transfer coefficient of console is higher than fan shaped hole, while the aerodynamic loss is significantly less than fan shaped hole. Chen et al (Chen et al., 2021) developed a prediction model to predict 2-Dimensional film cooling effectiveness of cooling hole, which can be used on the cooling design and optimization. Besides, there are lots of novel hole shapes proposed in literature and improved the cooling effectiveness (Kusterer et al., 2007; Yao et al., 2014; Kalghatgi and Acharya, 2015).

Besides the film cooling effectiveness, the thermal-mechanical constraint should be considered when apply a new cooling hole, as drilling holes influence the blade strength significantly. Mao et al (Mao et al., 2013) studied the crack evolution on a crystal plate specimen with a single cooling hole. By comparing experiment and simulation results, they found that, around the cooling hole, the stress concentrations were developed in four directions, in which the crack may propagate. For multi holes interaction, Wang et al (Wang et al., 2019) found that the interference between holes would accelerate formation of inter-hole slip zone and accumulation of plastic strain, which is damaging for specimen. Li et al (Li et al., 2019) investigated effect of microstructure around cooling hole on crack development, which result shows that, the

metallic carbides have influence on crack evaluation. In order to predict fatigue lifetime with cooling holes, Wen et al (Wen et al., 2018) proposed a model, which uses the damage parameter of maximum resolved shear stress/stain, and this model is suitable with both single and multi holes.

Meanwhile, inhomogeneous temperature distribution around cooling hole caused by coolant would lead to additional thermal stress on blade. Skamniotis et al (Skamniotis and Cocks, 2021*a*,*b*; Skamniotis et al., 2021) carried out a series research on the thermal stress analysis of double wall transpiration cooling (DWTC) systems. They considered the effect of wall spacing, wall thickness ratio and other parameters on the DWTC and found that large hole inclinations could lead to extreme stress concentration factors and thinner inner wall could reduce the critical compressive stress in the hot wall. Li et al (Li et al., 2023) investigated how the hole inclination angle and blowing ratio would influence the cooling system stress. They found that, when increase the blowing ratio the maximum thermal stress will also increase. Jiang et al (Jiang et al., 2019) numerically analyzed a film cooling system with thermal barrier coating and found that the film cooling caused a steep thermal gradient and led high stress concentration around the cooling hole.

The effect of hole geometry on the cooling performance has received a lot of attention, while the structure strength of the cooling system, especially of the shaped hole only get limited research. In this paper, the cooling effectiveness and the thermal stress of different cooling hole are investigated, trying to find out the relationship among them.

NUMERICAL SETUP

In this paper, five geometry parameters, including cylinder section length (L_m), expansion angles at the leading edge (β_{fwd}) and the trailing edge (β_{bwd}), the lateral angle (β_{lat}) and the radius of four edges inside diffuser (R), are chosen to obtain the results of different fan shaped cooling holes, as shown in Figure 1, while the cylinder part diameter (D) is fixed at 1 mm, the pitch size is 6 mm, the inclination angle is 30° and the total length of cooling hole (L) is 6 mm. The parameters value range is shown in Table 1. Large ranges are used to get as more holes' results as possible. To reduce the total time of simulation while keep the results covering the value range well, DOE (Design of Experiments) sample method is used. The DOE sample method needs $10n$ samples, in which n is the number of variable parameters, to cover the value range. In this paper, n equals to 5, so 50 samples are generated by pyDOE.

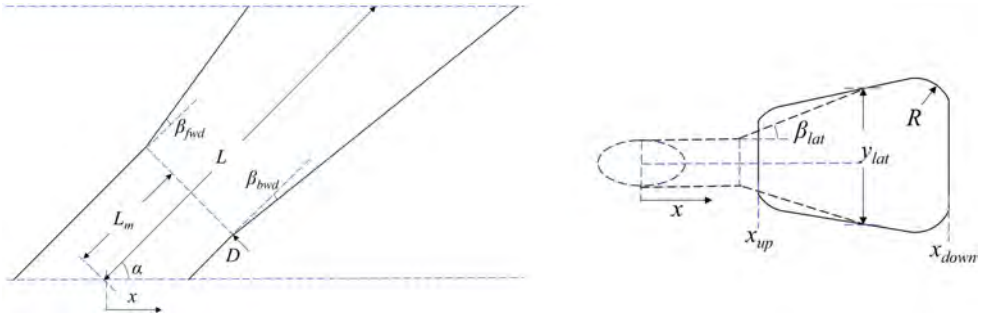

Figure 1 Cooling hole geometry parameters.

Table 1 Parameters value range.

Parameter name	L_m/L / [-]	β_{fwd} / [°]	β_{bwd} / [°]	β_{lat} / [°]	R/D / [-]
Range	0.35 ~ 0.75	-4 ~ 25	-5 ~ 25	2 ~ 18	0 ~ 0.5

For every single film cooling hole, to evaluate both its film cooling effect and structure strength, CFD (computational fluid dynamics) simulation and FEA (Finite Element Analysis) simulation are used. The geometry sizes of the simulation domains are shown in Figure 2, in which the blank part is fluid domain and grey part is solid domain. Although fluid and solid domain are displayed together here, the CFD and FEA simulation are separated. The temperature boundary conditions used in solid domain are interpolated based on CFD simulation result, which will be explained at Strength Setup section.

CFD Setup

In CFD simulation, Ansys Fluent is used to generated calculation mesh and get the temperature result at the main wall of the fluid domain. Figure 3 shows half of fluid mesh generated by Ansys Fluent with poly-hexcore hybrid mesh type. The first layer heights from main wall, coolant wall and hole are 0.001 mm, making y^+ of concerned region smaller than 1. The Realizable $k-\varepsilon$ model with standard wall functions is used in the Fluent solver. The main flow inlet temperature is 1600 K and the velocity is 150 m/s, while the coolant inlet temperature is 800 K and the blow ratio is 1.0. The outlet boundary condition is 1 atm. The fluid used in simulation is air, with constant fluid properties. All walls are adiabatic and main wall, coolant wall and hole are no slip walls, while the others are slip walls. The side boundaries are symmetry boundaries. Four

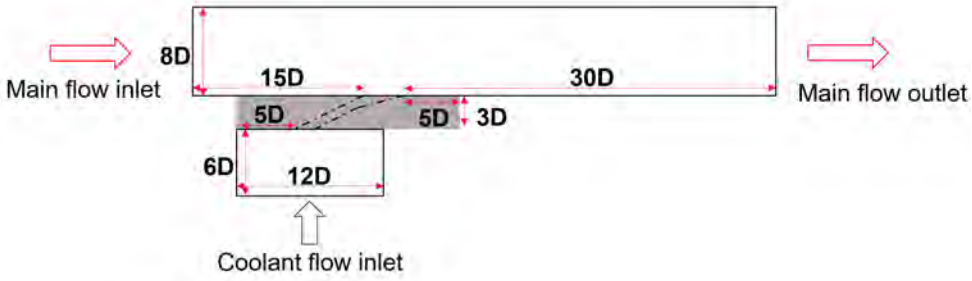

Figure 2 Simulation domains (D=1 mm).

mesh sizes are generated for the mesh independent test, which contents 1, 2, 4, 8 million mesh nodes, respectively. The lateral averaged film cooling effectiveness are compared, shown in Figure 4. Based on mesh independent test, mesh nodes number around 4 million is used.

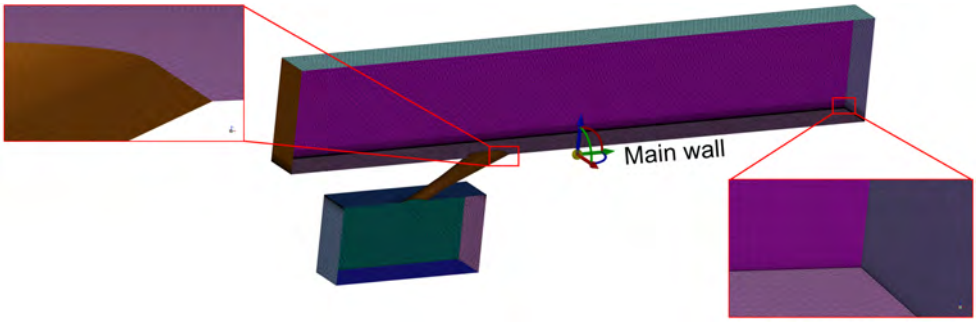

Figure 3 Fluid mesh.

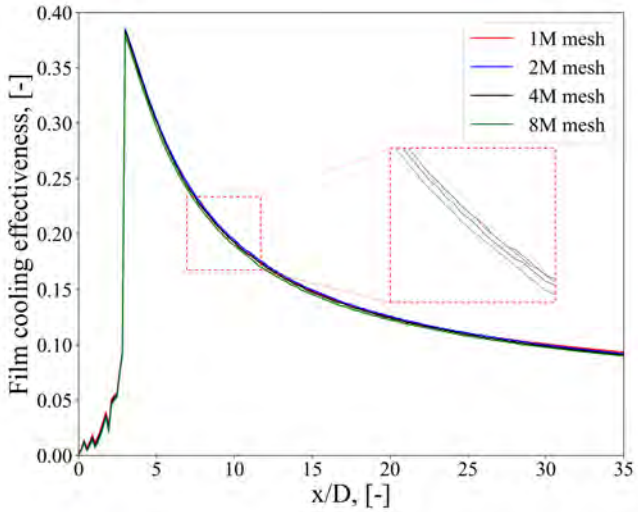

Figure 4 Mesh independent test.

Strength Part

We use the Ansys Workbench to carry on the FEA simulation. The structure mesh is also generated by Ansys Fluent, while with hexcore mesh type, as shown in the Figure 5. The temperature of the main wall and the hole are interpolated with the result from CFD simulation, which are not uniform and may impact the structure strength result. The coolant wall temperature is set to be same as the coolant air, 800 K, as the temperature is almost uniform in the CFD result. The material used for simulation is Titanium alloy, which is a base material in Ansys Workbench. To get temperature distribution of inner solid domain, a thermal analysis will be done first with Ansys Workbench, and then the stress analysis is applied to get the thermal stress. In this paper, we only considered the thermal stress influence, so there is no additional pressure force applied

to the solid domain. For the wall constraint, it is difficult to define what constraint should be used, since cooling hole could be applied at many places in turbine. As only thermal stress caused by uneven temperature is considered in this paper, the upstream side of the solid domain are fixed, as shown in the Figure 5, so that the solid domain could expand freely(Li et al., 2023).

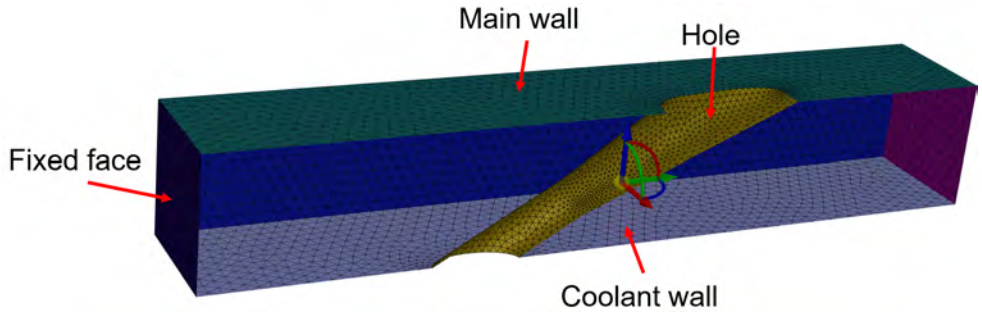

Figure 5 Solid mesh.

RESULTS AND DISCUSSION

We plan to simulate 50 samples of different hole shape, as mentioned above. However, there are some samples failed to generate the mesh, so at last 46 samples were used to obtain the relation between hole shape and cooing effect, as well as structure strength. A typical shaped hole, 7-7-7 shaped hole, is chosen to be a baseline case for comparison of results in this paper.

The hole shape samples are generated based on DOE method, which means all the five parameters will change at the same time. So the control variable method is not suitable in this case. It is very hard to distinguish how a specific parameter will affect the result. As a result, a composited variable, at last combines most parameters, is needed to find the relationship between parameters and results.

Film Cooling Effects

To evaluate the film cooling effect, the area average temperature (T_{aa}) of a part of the main wall, from the cooling hole exit to the end of the channel, is used. The T_{aa} range of all these samples is from 1459 to 1519 K, while result of the baseline case is 1477 K. Figure 6 shows the film cooling effectiveness results on the main wall of the best, baseline and worst sample, as well as the middle sections of these holes' geometry. From Figure 6 we can find that, the best hole has widest lateral expansion distance, making the coolant air expanding better than the baseline shape along the lateral side. The lateral expansion distance of the worst one is narrowest among these three holes, leading to a lower coolant coverage, to some extent.

In the mean time, it should be noticed that the β_{fwd} of the worst hole is larger and the β_{bwd} is smaller, which make its jet angle larger than the other two. With larger jet angle, the coolant air more likely flows away from the main wall, leading to a poor coverage at the main wall. Comparing the center plane film cooling effectiveness (η) distribution in the Figure 7, the above phenomenon can be found. In Figure 7, the coolant air from the worst hole reaches higher position than the other two, which means the coolant air flows away from the main wall.

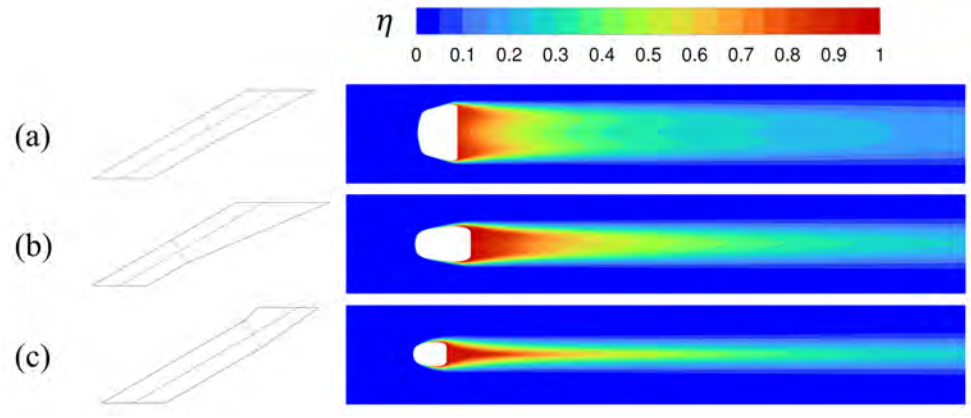

Figure 6 Film cooling effectiveness results on the main wall. (a) Best; (b) Baseline; (c) Worst.

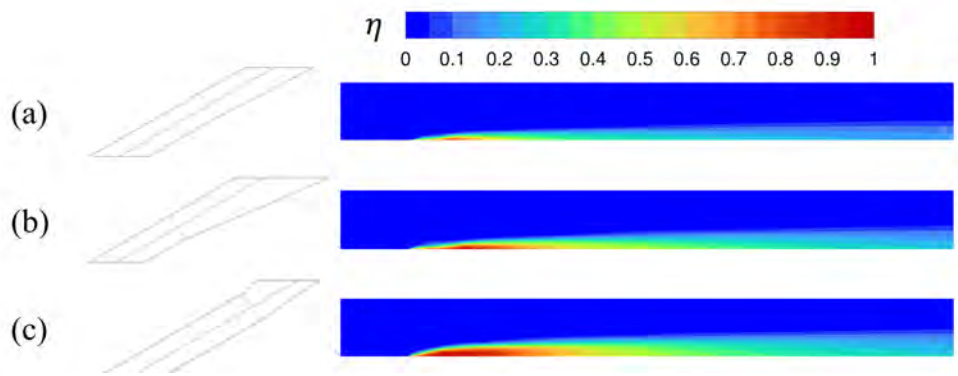

Figure 7 Film cooling effectiveness results on the center plane. (a) Best; (b) Baseline; (c) Worst.

As mentioned above, a composited variable is needed to find the general trend between input and output. Based on the basic parameters used for generating cooling hole geometry, some macro geometry parameters can be obtained, including the start (x_{up}) and end position (x_{down}), as well as the lateral width (y_{lat}) of the cooling hole at the main wall, as shown in Figure 1. In general, a two-dimensional slot hole has better cooling performance, so the guideline of developing this variable is to judging the degree of similarity with slot hole. For example, with smaller $x_{down} - x_{up}$, the hole exit will be narrower, and with larger y_{lat}, the hole lateral expansion will be larger, both making the cooling hole more like a slot hole. Finally, a composited variable, C_1, is defined as follow:

$$C_1 = \frac{x_{down} + x_{up}}{x_{down} - x_{up}} * \frac{y_{lat}}{6D} * (1 - \frac{L_m}{L}) \tag{1}$$

This variable is suitable as a comprehensive parameter to represent the hole geometry, since it is a dimensionless variable and include all the basic parameters except R. Figure 8 shows the relationship between the composited variable C_1 and the area average temperature T_{aa}, in which the black dots represent the sample results and the red star represents the baseline case result. From Figure 8, we can find that: when C_1 is small, the area average temperature tends to be high, like shown in the upper right of Figure 8, while when the C_1 is large, the area average temperature can be low. The Pearson correlation coefficient between C_1 and T_{aa} is -0.789, which means they have a negative correlation. To get a low area average temperature, we need a large C_1, and from the definition of C_1, large flow side and lateral side expansion, as well as small start and end position different, result a large C_1.

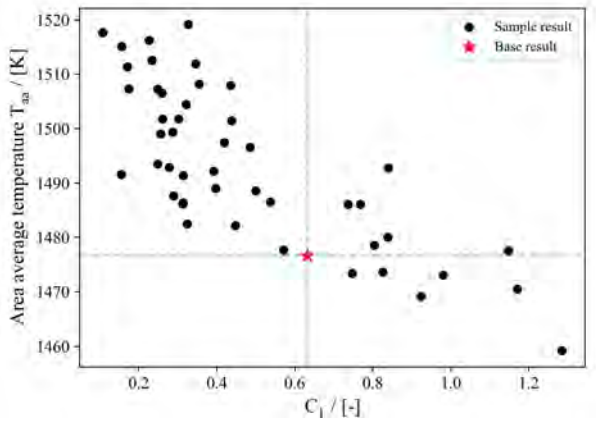

Figure 8 Relationship between C_1 and T_{aa}

Structure Strength

The maximum value of von Mises stress ($\sigma_{v,max}$) is used to analysis how the hole shape will affect the structure strength of the solid part. Only the center part of the solid domain is used to get the von Mises stress cutting 3 D at both sides, otherwise the fixed boundary condition face may has great influence on the result. The $\sigma_{v,max}$ range of all samples is from 537.5 to 1569 MPa, and the result of baseline case is 791.6 MPa. Figure 9 shows the comparison among the lowest and highest stress sample, as well as the baseline sample results and their temperature distribution. The maximum values are

all on the upside surface of the cooling hole in Figure 9, where the temperature gradient is very large. Comparing with the other two cases, the highest $\sigma_{v,max}$ sample has the narrowest upside of the hole exit, which may lead to a higher local stress, while the case with large hole exit has lowest $\sigma_{v,max}$, even the temperature is higher than the baseline case.

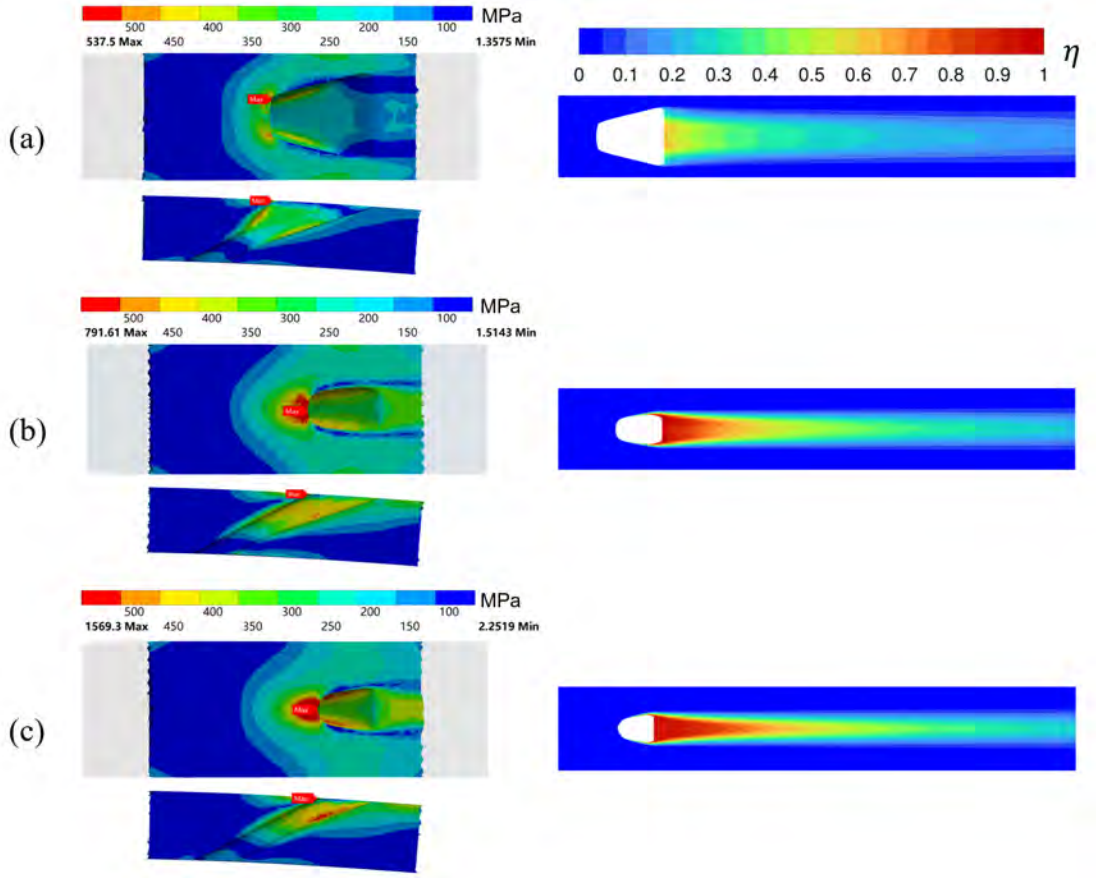

Figure 9 Von Mises stress and film cooling effectiveness results (a: Lowest $\sigma_{v,max}$; b: Baseline; c: Highest $\sigma_{v,max}$).

To find the relationship between hole geometry parameters and the structure strength, we also need a composited variable to represent the hole geometry. As there are few literatures about strength of cooling hole geometry, so there is no clear guideline when developing this variable. By trying different combinations and verifying their effect, a suitable variable, C_2, is found luckily, which is defined as follow:

$$C_2 = \frac{x_{up} + x_{down}}{x_{down}} * \frac{y_{lat}}{6D} * \frac{1}{cos(\beta_{bwd})} * (1 - \frac{L_m}{L}) \tag{2}$$

C_2 is also a dimensionless variable and includes most basic parameters. The relationship between C_2 and $\sigma_{v,max}$ is shown in Figure 10, in which we can find that they have a negative correlation. The Pearson correlation coefficient is -0.731. If the C_2 of one hole shape is large, the maximum value of von Mises stress trend to be small.

Optimal Hole Structure

Based on above results, we get two composited variables, C_1 and C_2. The definitions of C_1 and C_2 are very similar and can be large at the same time, which makes the area average temperature and the von Mises stress small for gas turbine application. Within the cooling hole shape parameter design range, we can choose some suitable parameter values, which make these two variables large at the same time.

It is a dual objective optimization to get parameter values to make C_1 and C_2 be large at the same time. With Python code, the Pareto optimality samples can be found, which have both large C_1 and C_2. We use one of them to generate cooling hole and simulate its cooling effect and structure strength. The basic parameters of the chosen one is list in Table 2.

Figure 11 shows the C_1 and C_2 of all the samples results, including baseline case and optimized case, and the $\sigma_{v,max}$ and T_{aa} shown in Figure 12. In Figure 11, we can find that, the optimized case has the highest C_1 and C_2, which should result in lower $\sigma_{v,max}$ and T_{aa} according to above conclusions. When check the Figure 12, the optimized case indeed has lowest T_{aa} and lower $\sigma_{v,max}$, comparing with other samples. To a certain extent, this result verifies that the above composited variables C_1 and C_2 are suitable to represent hole geometry when consider the cooling effect and the structure strength. Figure 13

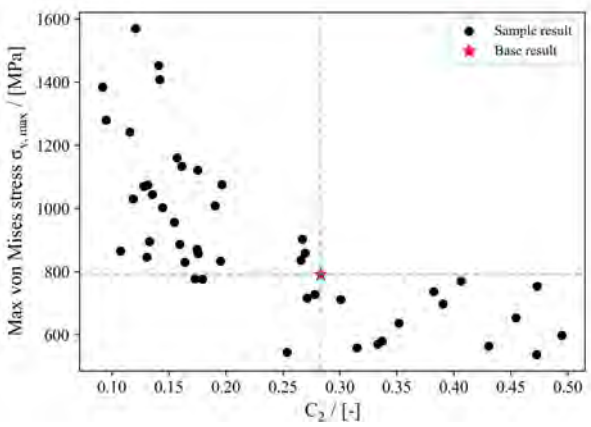

Figure 10 Relationship between C_2 and $\sigma_{v,max}$.

Table 2 Parameters value of the optimized case.

Parameter name	L_m/L / [-]	β_{fwd} / [°]	β_{bwd} / [°]	β_{lat} / [°]	R/D / [-]	C_1 / [-]	C_2 / [-]
Value	0.353	1.992	1.685	16.542	0.366	1.499	0.576

shows the von Mises stress and the temperature distributions of the optimized case, which perform better than the baseline case, as well as most of the samples.

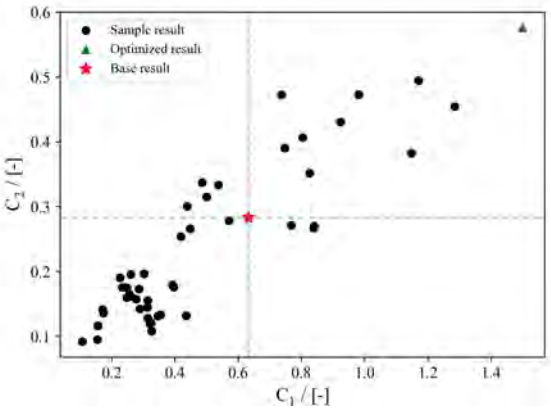

Figure 11 Distribution of C_1 and C_2.

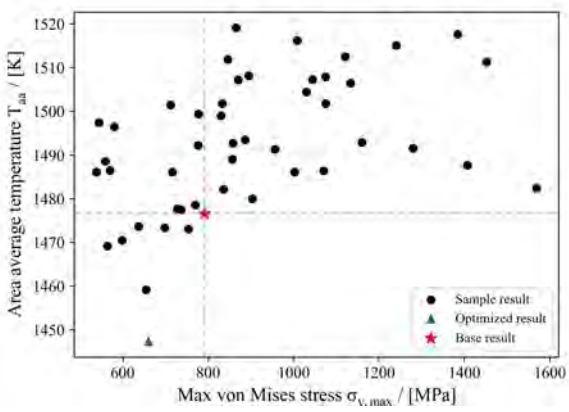

Figure 12 Distribution of between T_{aa} and $\sigma_{v,max}$.

CONCLUSIONS

In this paper, five basic parameters are chosen to be changed to generate 46 different cooling hole shapes. The cooling effects and structure strength are analyzed to find the relationship between the basic parameters and the results and two composited variables, C_1 and C_2 are used to represent the hole geometry. The main conclusions are as follow:

The composited variables C_1 and C_2 has obvious negative correlation with the area average temperature (T_{aa}) and the maximum von Mises stress ($\sigma_{v,max}$) respectively, so they are suitable to represent the hole geometry.

To get low T_{aa} and low $\sigma_{v,max}$, the C_1 and C_2 value should be large. The definition of C_1 and C_2 are similar, so it is possible to make them large at the same time, which means the cooling hole can have superior cooling effect while keep the structure strength good enough. The optimized case also shows the possibility.

In the future research, more basic parameters and larger value range should be evaluate to improve the composited variables to make them representing cooling effect and structure strength better.

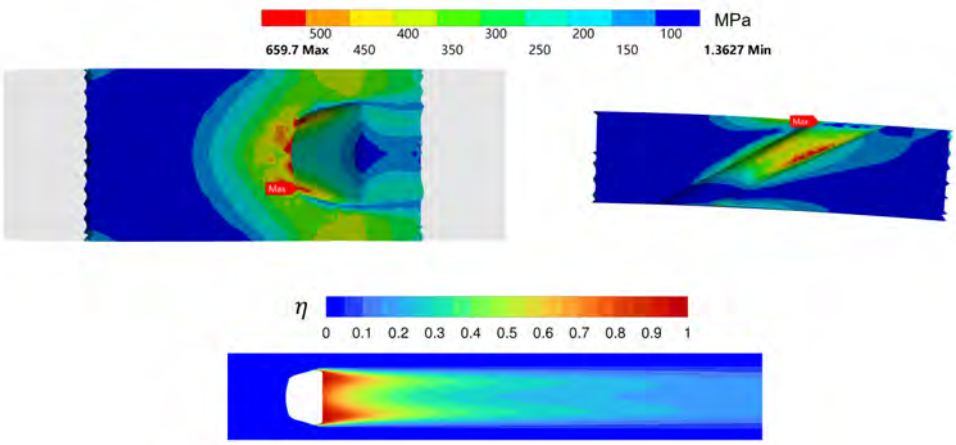

Figure 13 Von Mises stress and film cooling effectiveness results of optimized case.

NOMENCLATURE

C_1	=	composited variable 1	C_2	=	composited variable 2
CFD	=	Computational Fluid Dynamics	D	=	cooling hole diameter, mm
FEA	=	Finite Element Analysis	L	=	total length of cooling hole, mm
L_m	=	cylinder section length, mm	M	=	blow ratio, $(\rho_c U_c)/(\rho_\infty U_\infty)$
R	=	radius of interior edge rounding, mm	T_{aa}	=	area average temperature, K
T_{aw}	=	wall temperature, K	T_c	=	coolant inlet temperature, K
T_∞	=	main flow inlet temperature, K	U_c	=	coolant inlet velocity, m/s
U_∞	=	main flow inlet velocity, m/s	x_{down}	=	hole exit end position, mm
x_{up}	=	hole exit start position, mm	y_{lat}	=	lateral width, mm
β_{bwd}	=	trailing edge expansion angle, °	β_{fwd}	=	leading edge expansion angle, °
β_{lat}	=	lateral angle, °	η	=	cooling effectiveness, $(T_\infty - T_{aw})/(T_\infty - T_c)$
$\sigma_{v,max}$	=	maximum von Mises stress, MPa			

ACKNOWLEDGMENTS

This work is supported by the National Natural Science Foundation of China [Grant No. 52276031] and National Science and Technology Major Project [J2019-III-0007-0050].

References

Chen, Z., Li, Y., Su, X. and Yuan, X. (2021), 'Scalar diffusion equation-based model to predict 2-dimensional film cooling effectiveness of a shaped hole', *Journal of Turbomachinery* **143**(4).

Goldstein, R., Eckert, E. and Burggraf, F. (1974), 'Effects of hole geometry and density on three-dimensional film cooling', *International Journal of heat and mass transfer* **17**(5), 595–607.

Gritsch, M., Colban, W., Schär, H. and Döbbeling, K. (2005), 'Effect of hole geometry on the thermal performance of fan-shaped film cooling holes'.

Jiang, J., Jiang, L., Cai, Z., Wang, W., Zhao, X., Liu, Y. and Cao, Z. (2019), 'Numerical stress analysis of the tbc-film cooling system under operating conditions considering the effects of thermal gradient and tgo growth', *Surface and Coatings Technology* **357**, 433–444.

Kalghatgi, P. and Acharya, S. (2015), 'Improved film cooling effectiveness with a round film cooling hole embedded in a contoured crater', *Journal of Turbomachinery* **137**(10), 101006.

Kusterer, K., Bohn, D., Sugimoto, T. and Tanaka, R. (2007), 'Double-jet ejection of cooling air for improved film cooling'.

Li, H., Zhang, D., You, R., Zou, Y. and Liu, S. (2023), 'Numerical investigation of the effects of the hole inclination angle and blowing ratio on the characteristics of cooling and stress in an impingement/effusion cooling system', *Energies* **16**(2), 937.

Li, Z., Wen, Z., Gu, S., Pei, H., Gao, H. and Mao, Q. (2019), 'In-situ observation of crack initiation and propagation in ni-based superalloy with film cooling holes during tensile test', *Journal of Alloys and Compounds* **793**, 65–76.

Mao, H., Wen, Z., Yue, Z. and Wang, B. (2013), 'The evolution of plasticity for nickel-base single crystal cooled blade with film cooling holes', *Materials Science and Engineering: A* **587**, 79–84.

Sargison, J., Guo, S., Oldfield, M., Lock, G. and Rawlinson, A. (2002*a*), 'A converging slot-hole film-cooling geometry—part 1: low-speed flat-plate heat transfer and loss', *J. Turbomach.* **124**(3), 453–460.

Sargison, J., Guo, S., Oldfield, M., Lock, G. and Rawlinson, A. (2002*b*), 'A converging slot-hole film-cooling geometry—part 2: transonic nozzle guide vane heat transfer and loss', *J. Turbomach.* **124**(3), 461–471.

Skamniotis, C. and Cocks, A. C. (2021*a*), '2d and 3d thermoelastic phenomena in double wall transpiration cooling systems for gas turbine blades and hypersonic flight', *Aerospace Science and Technology* **113**, 106610.

Skamniotis, C. and Cocks, A. C. (2021*b*), 'Designing against severe stresses at compound cooling holes of double wall transpiration cooled engine components', *Aerospace Science and Technology* **116**, 106856.

Skamniotis, C., Courtis, M. and Cocks, A. C. (2021), 'Multiscale analysis of thermomechanical stresses in double wall transpiration cooling systems for gas turbine blades', *International Journal of Mechanical Sciences* **207**, 106657.

Wang, J., Liang, J., Wen, Z., Yang, Y. and Yue, Z. (2019), 'The inter-hole interference on creep deformation behavior of nickel-based single crystal specimen with film-cooling holes', *International Journal of Mechanical Sciences* **163**, 105090.

Wen, Z., Pei, H., Yang, H., Wu, Y. and Yue, Z. (2018), 'A combined cp theory and tcd for predicting fatigue lifetime in single-crystal superalloy plates with film cooling holes', *International Journal of Fatigue* **111**, 243–255.

Yao, Y., Zhang, J.-z. and Tan, X.-m. (2014), 'Numerical study of film cooling from converging slot-hole on a gas turbine blade suction side', *International Communications in Heat and Mass Transfer* **52**, 61–72.

Yu, Y., Yen, C.-H., Shih, T.-P., Chyu, M. and Gogineni, S. (2002), 'Film cooling effectiveness and heat transfer coefficient distributions around diffusion shaped holes', *J. Heat Transfer* **124**(5), 820–827.

Zhang, J., Zhang, S., Chunhua, W. and Xiaoming, T. (2020), 'Recent advances in film cooling enhancement: A review', *Chinese Journal of Aeronautics* **33**(4), 1119–1136.